STD-R-2694

Physical and Biological Descriptors for Ocean Bubbles and Acoustic Surface Backscatter

October 1997

SUBMARINE TECHNOLOGY DEPARTMENT

THE JOHNS HOPKINS UNIVERSITY
APPLIED PHYSICS LABORATORY
Johns Hopkins Road, Laurel, Maryland 20723-6099

Operating under Contract N00014-97-1-0075

REPORT DOCUMENTATION PAGE

Form Approved
OMB No. 0704-0188

1. AGENCY USE ONLY *(Leave blank)*	2. REPORT DATE	3. REPORT TYPE AND DATES COVERED
	30 Sep 97	Final: 1 Oct 94 through 30 Sep 97

4. TITLE AND SUBTITLE

Physical and Biological Descriptors for Ocean Bubbles and Acoustic Surface Backscatter

5. FUNDING NUMBERS

N00014-95-1-0078
and
N00014-97-1-0075

6. AUTHOR(S)

Jeffrey L. Hanson

7. PERFORMING ORGANIZATION NAME(S) AND ADDRESS(ES)

The Johns Hopkins University
Applied Physics Laboratory
Johns Hopkins Road
Laurel, Maryland 20723-6099

8. PERFORMING ORGANIZATION REPORT NUMBER

STD-R-2694

9. SPONSORING/MONITORING AGENCY NAME(S) AND ADDRESS(ES)

Department of the Navy
Office of Naval Research
Ocean Acoustics Code 3210A
800 N. Quincy St.
Arlington, VA 22217

10. SPONSORING/MONITORING AGENCY REPORT NUMBER

11. SUPPLEMENTARY NOTES

12a. DISTRIBUTION/AVAILABILITY STATEMENT

Approved for Public Release
Distribution is Unlimited

12b. DISTRIBUTION CODE

13. ABSTRACT *(Maximum 200 words)*

Processes related to the supply, mixing, and removal of ocean bubbles and their impact on low frequency (0-1000 Hz) acoustic surface scattering strength (SSS) in the upper ocean have been investigated. A key finding is that gross site-to-site differences between Critical Sea Test and Chapman-Harris SSS observations are explained by the mean ocean temperature, biological productivity, and wave conditions at each site. Furthermore, wave energy dissipation rate, estimated from wave spectra using wave energy flux considerations, was found to be a better descriptor for ocean whitecaps, related to upper ocean bubble supply, than wind speed. These results demonstrate that a model could be developed for estimating SSS statistics in coastal areas using readily available (by satellite and operational models) environmental inputs.

14. SUBJECT TERMS

acoustic surface scatter, acoustic backscatter, ocean bubbles, whitecaps, wave dissipation, wave partitioning, biological productivity

15. NUMBER OF PAGES

20

16. PRICE CODE

17. SECURITY CLASSIFICATION OF REPORT	18. SECURITY CLASSIFICATION OF THIS PAGE	19. SECURITY CLASSIFICATION OF ABSTRACT	20. LIMITATION OF ABSTRACT
UNCLASSIFIED	UNCLASSIFIED	UNCLASSIFIED	UL

REPRODUCTION QUALITY NOTICE

This document is the best quality available. The copy furnished to DTIC contained pages that may have the following quality problems:

- Pages smaller or larger than normal.
- Pages with background color or light colored printing.
- Pages with small type or poor printing; and or
- Pages with continuous tone material or color photographs.

Due to various output media available these conditions may or may not cause poor legibility in the microfiche or hardcopy output you receive.

☒ If this block is checked, the copy furnished to DTIC contained pages with color printing, that when reproduced in Black and White, may change detail of the original copy.

STD-R-2694

Physical and Biological Descriptors for Ocean Bubbles and Acoustic Surface Backscatter

Final Report for Office of Naval Research: N00014-95-1-0078/N00014-97-1-0075

October 1997

Jeffrey L. Hanson

SUBMARINE TECHNOLOGY DEPARTMENT

THE JOHNS HOPKINS UNIVERSITY
APPLIED PHYSICS LABORATORY
LAUREL, MARYLAND

This page intentionally left blank.

CONTENTS

This page intentionally left blank.

LIST OF ILLUSTRATIONS

LIST OF TABLES

ABBREVIATIONS & ACRONYMS

ASREX	Acoustic Surface Reverberation Experiment
chl	Chlorophyll Concentration
CST	Critical Sea Test
CZCS	Coastal Zone Color Scanner
h_s	Significant Wave Height
ONE	Ogden-Nicholas-Erskine Surface Scatter Model
SSS	Surface Scattering Strength
SSSe	SSS Prediction Error
sst	Sea Surface Temperature
U_{10}	Wind Speed at 10-m Elevation

This page intentionally left blank.

1. Summary

Processes related to the supply, mixing, and removal of ocean bubbles and their impact on low-frequency (0-1000 Hz) acoustic surface scattering strength (SSS) in the upper ocean have been investigated. A key finding is that gross site-to-site differences between Critical Sea Test (CST) and Chapman-Harris SSS observations are explained by the mean ocean temperature, biological productivity, and wave conditions at each site. Furthermore, wave energy dissipation rate, estimated from wave spectra using wave energy flux considerations, was found to be a better descriptor for ocean whitecaps, related to upper ocean bubble supply, than wind speed. These results demonstrate that a model could be developed for estimating SSS statistics in coastal areas using readily available (by satellite and operational models) environmental inputs.

2. Background

As an important element of underwater sonar performance, SSS measurements have been made in a variety of oceanographic conditions by numerous investigators. The recent series of CST experiments (1988-1992) has provided a rich set of observations, obtained with a consistent technique, in six different environments. The calibrated CST results can be readily compared with earlier measurements such as those of Chapman and Harris obtained North of Bermuda in 1962 (*Reference 1*).

Surface scattering results from the CST program have been reviewed in a series of reports by M. Nicholas, P. Ogden, F. Erskine, and R. Gauss of NRL and F. Henyey and E. Thorsos of APL/UW. The CST results most relevant to our study are listed here:

- SSS is strongly linked to short-term (~ 1 h) wind history.
- Supporting environmental data suggest that SSS is more closely associated with tenuous bubble clouds than with breaking wave events.
- Acoustic model comparisons with CST results indicate that near-surface (~ 1-3 m) microbubbles, entrained by wave orbital motions, contribute most to SSS.
- Significant differences (6-7 dB) are noted between CST-4 and CST-7 SSS results at similar wind-forcing conditions (see Figure 1). Unexplained differences also exist between other CST data sets and with Chapman-Harris.
- CST 1, 2, 3, 4, 5, and 7 results used to construct NRL Ogden-Nicholas-Erskine (ONE) empirical SSS model. Environmental input is the 1-hr backaveraged wind speed.

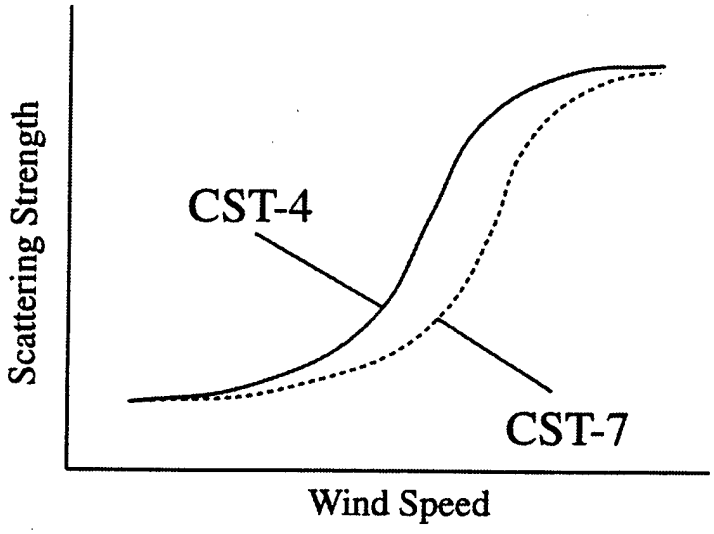

Actual values between these sites differ by as much as 8 dB. Adapted from Nicholas, M., P. M. Ogden, and F. T. Erskine, Improved Empirical Descriptions for Acoustic Surface Backscatter in the Ocean, submitted to *IEEE J. Oce. Engineering.*

Figure 1 Scattering Strength Differences Between CST-4 and CST-7

A crucial issue remaining from the CST program is explanation of the large site-to-site differences in SSS. It was anticipated that results from the Acoustic Surface Reverberation Experiment (ASREX), conducted west of Bermuda over a 3-month period during the 1993-1994 winter storm season, would identify the environmental factors missing from the Chapman-Harris and ONE SSS models. Unfortunately, calibrated SSS levels from ASREX are not yet available for direct comparison with the CST results. However, the extended analysis of CST observations reported here has led to a possible explanation for site-to-site differences in SSS.

3. Research Objectives

Our hypothesis is that site-to-site variations in SSS are a result of physical and biological factors related to the supply, mixing, and removal of bubbles in the upper ocean. As the wind speed input of SSS models appears to adequately prescribe the local, short-term forcing of the upper ocean, the missing environmental factors must relate to the background setting of each site (swell, mixing, temperatures, dissolved gasses, surfactants, etc.). Hence, our primary research objectives were the following:

(1) Examine the influence of bubble-related environmental factors on SSS with particular emphasis on parameters linked to seasonal and geographic variations in near-surface bubble populations. The need to identify the 'missing link' for explaining site-to-site differences in SSS is recognized.

(2) Determine if surface wave descriptors can be used to augment or replace wind speed in air-sea process models such as those for air-sea gas flux (by bubble injection) and acoustic surface scatter.

4. Site-to-Site SSS Variability: An Explanation

4.1 SSS Prediction Errors

The NRL ONE model predicts SSS as a multiparameter function of frequency, grazing angle, and wind speed. Observation departures from ONE predictions, aside from measurement errors, result from environmental influences not well represented by wind speed alone. Here we isolate these departures by calculating the SSS prediction error

$$SSSe = SSS_{ONE} - SSS_{obs} \quad ,$$

with the 'ONE' and 'obs' subscripts referring to model predictions and observations, respectively.

The mean *SSSe* at 500 Hz for each of the CST and Chapman-Harris sites appears in Figure 2. The mean levels were calculated by averaging the prediction errors for each experiment over all wind speeds, all grazing angles > 10°, and over the frequency band 400-600 Hz. Error bars depict one standard deviation about the means. It is observed that CST-2 and CST-5 are over-predicted and that CST-1, CST-3, CST-4, and Chapman-Harris are under-predicted. The CST-7 values are close to zero; this is expected as CST-7 has contributed by far the most observations used for the ONE model fits. The differences between CST-4 and CST-7 levels have been particularly frustrating to the research

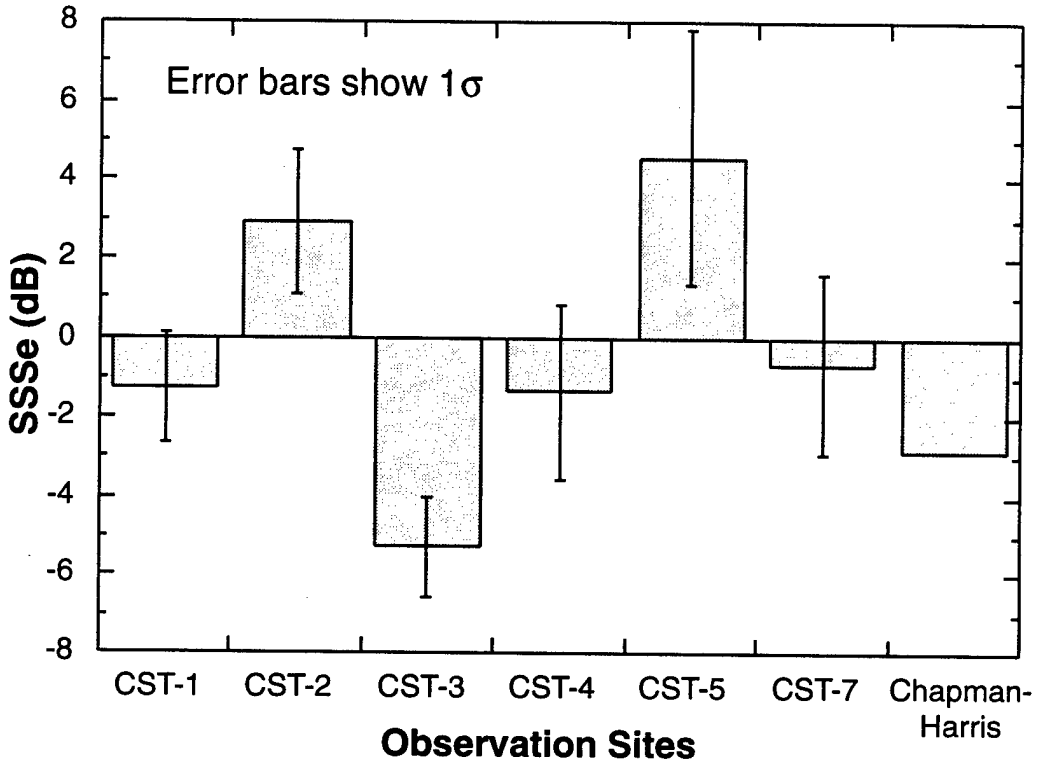

One standard deviation error bars are depicted.

Figure 2 Mean Surface Scatter Strength Prediction Error ($SSS_{ONE} - SSS_{obs}$) at 500 Hz

community as both experiments occurred in the Gulf of Alaska under similar wind and wave conditions (see Figure 1). Note that much larger differences exist between the remaining CST experiments, such as extreme differences between CST-3 and CST-5 of nearly 15 dB.

Our approach is to empirically relate *SSSe*, averaged over various frequency, grazing angle, and wind speed regimes, with the bubble-related environmental descriptors described in Section 4.2.

4.2 Environmental Descriptors

The ONE model wind speed input represents those environmental processes that influence surface scatter on short (hourly) time scales including surface wave development and the supply of bubbles by breaking waves. Missing from this model, however, are environmental descriptors for the background setting of each site, such as swell activity, mixed-layer temperature and depth, gas saturation, and surfactants. Both laboratory experiments and theoretical calculations have shown the importance of these background conditions on processes that supply, entrain, and remove bubbles from the upper ocean. The full complement of supporting environmental data collected during CST, combined with remote sensing products, has allowed a reasonable test of their importance to SSS.

The environmental descriptors found to be most important for site-to-site SSS variability appear in Table 1. Four factors are employed to describe bubble supply, entrainment, and removal processes in the ocean: wind speed (U_{10}), ocean temperature (*sst*), significant wave height (h_s), and chlorophyll concentration (*chl*). The importance of wind speed has already been demonstrated by its success in the various SSS model formulations (for example, Chapman-Harris and ONE).

Table 1
Environmental Descriptors for Surface Scatter by Bubbles

Bubble Issue	Process	Descriptor
Supply	Wave breaking	Wind speed Ocean temperature
Entrainment	Wave mixing	Wave height*
Removal	Gas dissolution	Ocean temperature Chlorophyll concentration

* Mean over entire test duration.

Significant wave height, averaged over the entire test duration, is employed here to represent the test site background energy setting and helps account for the effects of swell on wave breaking and mixing. It is expected that high-energy environments will support denser and deeper bubble populations.

Sea surface temperature (*sst*) significantly influences both the supply and removal of bubbles in the upper ocean. Both surface tension and viscosity are highest in cold water; this fact offers a preliminary explanation for reduced whitecap coverage in high latitudes (*Reference* 2). Water temperature also controls gas solubility. As less air can

dissolve in warmer water, we expect longer bubble lifetimes and hence, denser bubble populations with water temperature increases. CST surface temperatures were collected from 0.5-1.5 m depth and represent the typical ocean temperature within the near-surface bubble layer.

Phytoplankton biomass, characterized by remotely sensed chlorophyll concentrations, will also influence bubble lifetimes through two complementary mechanisms. First, surfactants secreted by biological communities are known to provide a stabilizing coating to seawater bubbles. Second, phytoplankton blooms can supersaturate the water with respect to oxygen and other atmospheric gases. Both of these effects will decrease the rate of bubble dissolution and promote larger bubble populations in biologically productive areas. This effect will be most important in nearshore and coastal waters where biological productivity is greatest.

Monthly mean phytoplankton pigment (chlorophyll) concentrations for the CST and Chapman-Harris sites were obtained from the Coastal Zone Color Scanner (CZCS) mission results on the World Wide Web (*http://seawifs.gsfc.nasa.gov/SEAWIFS.html*). This observation set covers 7.5 yr from October 1978 through June 1986. As the CST program did not begin until 1988, the CZCS pigment concentrations can only be used to represent typical conditions at each site. The North Atlantic Ocean images for the CST-1, CST-2, CST-3, and Chapman-Harris sites appear in Figure 3. Black areas on the images correspond to regions with no data, primarily due to ice and cloud cover. A dramatic increase in pigment concentration is observed at high latitudes between early spring and late summer, driven primarily by the availability of nutrients at high latitudes and the increase in light during the summer. Note in particular the large contrast between the CST-1 and CST-3 sites, and the highly variable nature of the CST-2 region. The North Pacific Ocean images for February (CST-7) and April (CST-4) appear in Figure 4. The effect of spring blooms in April is apparent with an increased level of productivity at the CST-4 site.

4.3 A Simple Check of Hypothesis

The dependence of gross site-to-site differences in surface scattering on the bubble-related environmental descriptors (Table 1) can be demonstrated with a few simple empirical tests. *SSSe* values from CST and the Chapman-Harris model were first averaged over three distinct frequency bands: 0-150 Hz, 400-600 Hz, and 800-1000 Hz. The data from all runs (individual observation sets) within each CST experiment were included in the averages as well as observations at all grazing angles > 10°. This gross averaging process was performed to minimize uncertainty due to random measurement errors, environmental patchiness, short-term variability, etc. Each experiment is now

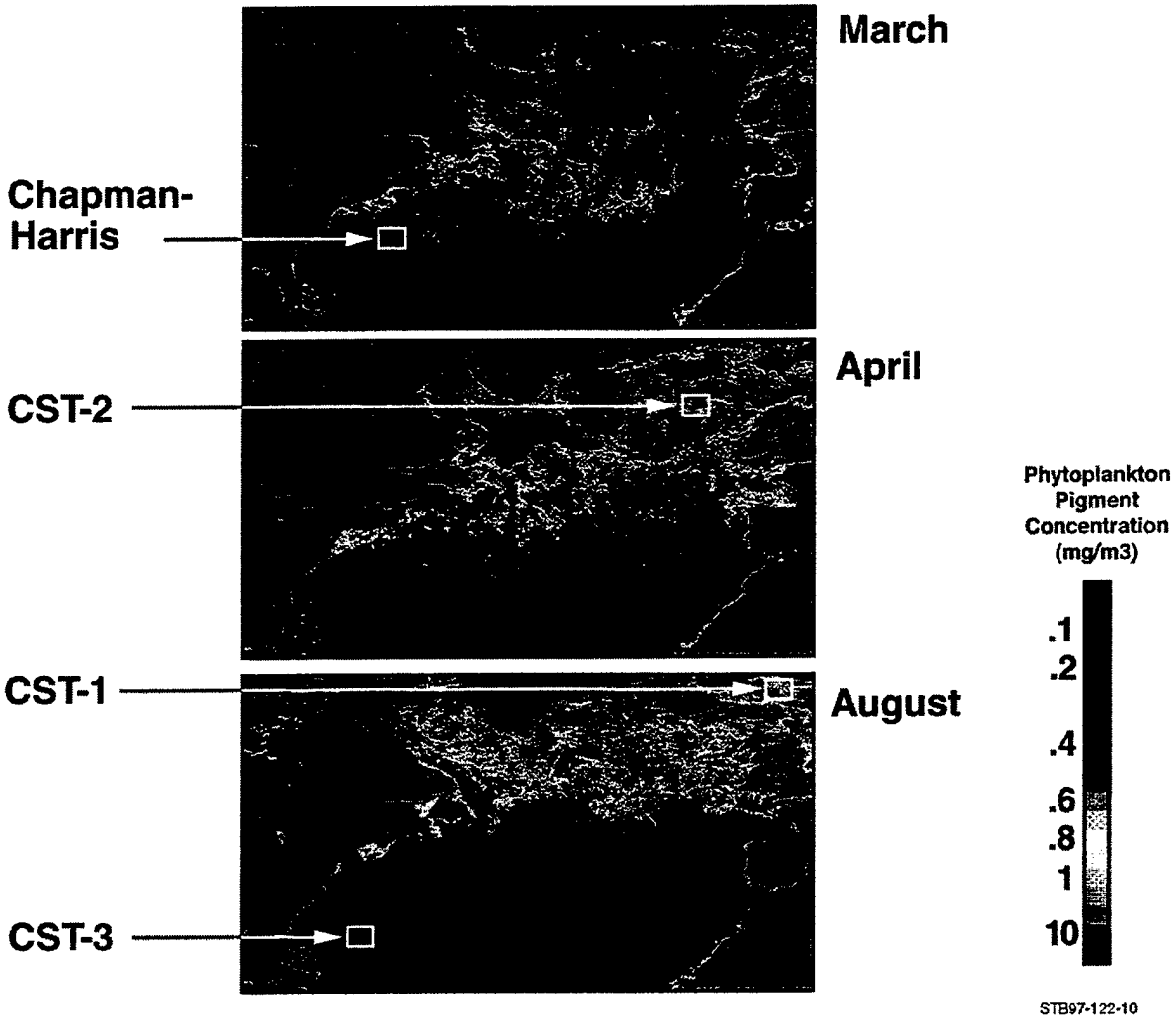

The SSS sites in this region are identified during the appropriate months. High nutrient concentrations in northern latitudes and increased sunlight in summer months result in an intensive high-latitude August bloom.

Figure 3 Mean Monthly Phytoplankton Pigment Concentration in the North Atlantic Ocean from the Coastal Zone Color Scanner

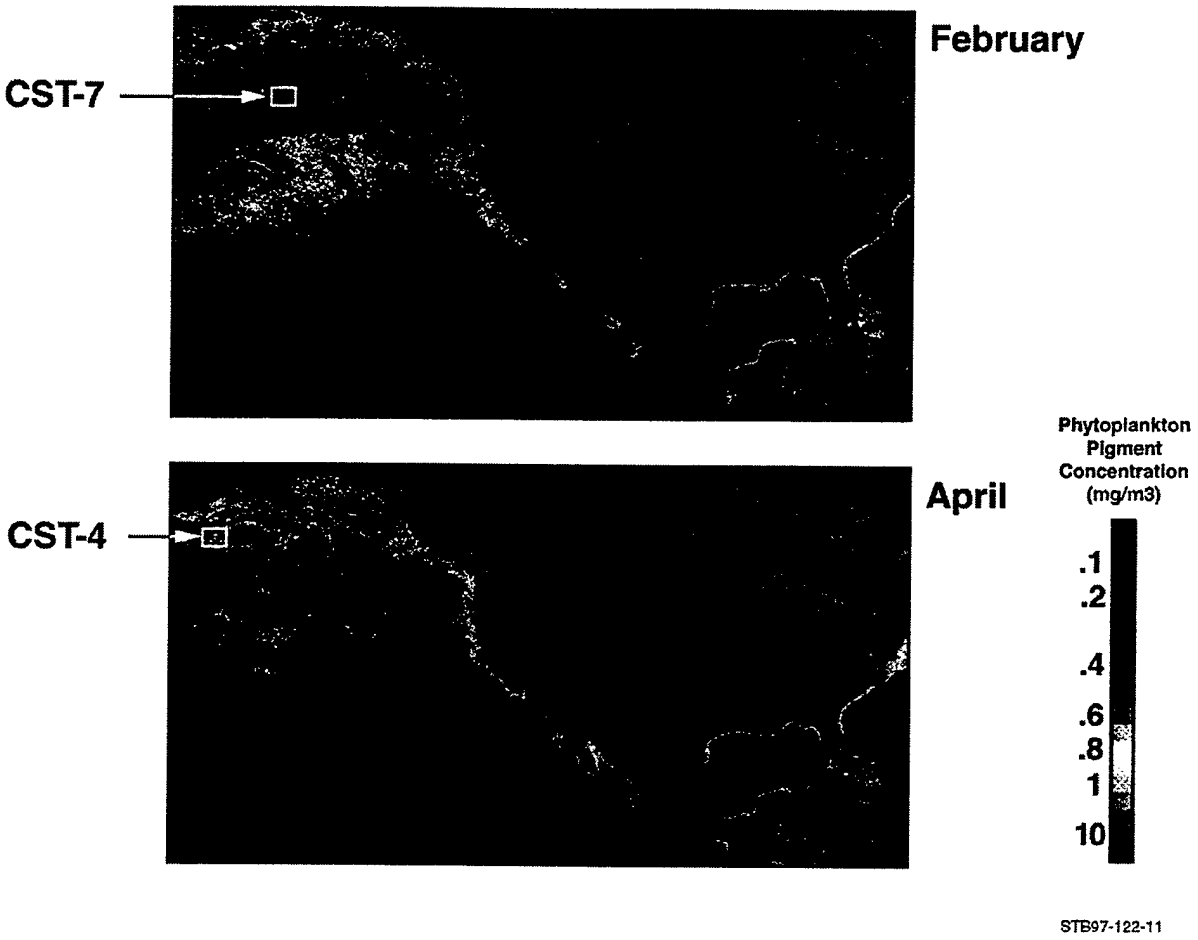

Cloud cover limited biological productivity during CST-7 in February (upper panel). Spring blooms likely influenced the water column properties during CST-4 in April (lower panel).

Figure 4 Mean Monthly Phytoplankton Pigment Concentration in the North Pacific Ocean from the Coastal Zone Color Scanner

conveniently described by the set of mean prediction errors, with corresponding baseline environmental descriptors, listed in Table 2. Note that wind speed values do not appear in Table 2. The objective is to identify additional environmental factors, beyond local wind effects, that contribute to SSS variability. It is assumed that wind speed contributions are adequately represented by the ONE model and are hence already 'accounted for' in the *SSSe* values.

Table 2
Mean Quantities Used for Investigation of Site-to-Site Differences

Source	h_s m	*sst* °C	*chl* mg/m^3	Mean *SSSe* (dB)		
				0 - 150 Hz	400 - 600 Hz	800 - 1000 Hz
CST 1	1.8	10.7	1.140	1.1	-1.3	- no data -
CST 2	2.5	8.3	0.516	4.8	2.9	3.2
CST 3	1.4	28.1	0.045	-2.3	-5.3	-0.1
CST 4	3.2	3.3	0.320	2.1	-1.4	0.8
CST 5	0.6	23.0	0.088	2.6	2.9	5.0
CST 7	3.3	5.5	0.176	1.0	-0.7	0.3
Chapman-Harris *	2.7	18.0	0.263	-1.5	-3.2	-2.6

* Chapman-Harris h_s and *sst* estimates obtained from *U.S. Navy Marine Climatic Atlas* CD-ROM.

The combined *SSSe* values depend on the three environmental descriptors in a manner that agrees with physical intuition. To facilitate display of these multidimensional results, we will first normalize the data with respect to the h_s dependence. Note that CST-2 and CST-4 are both cold water experiments with close *chl* values, and that CST-5 and CST-3 are both warm water experiments with close *chl* values. The *SSSe* differences between these experiment pairs should be dominated by h_s effects. This is verified by the *SSSe* vs. h_s plot of Figure 5. The differences between *SSSe* values of each experiment pair, and at each frequency range, are represented by a series of linear regressions. Note that all of the regressions are of similar slope with higher observed scattering strengths (relative to ONE predictions) as mean wave height increases. The regression slopes were averaged within frequency bands and used to produce wave-height normalized prediction errors (*SSSn*) for each of the observations in Table 2. The normalization is given by

$$SSSn = m(h_{sREF} - h_s) + SSSe,$$

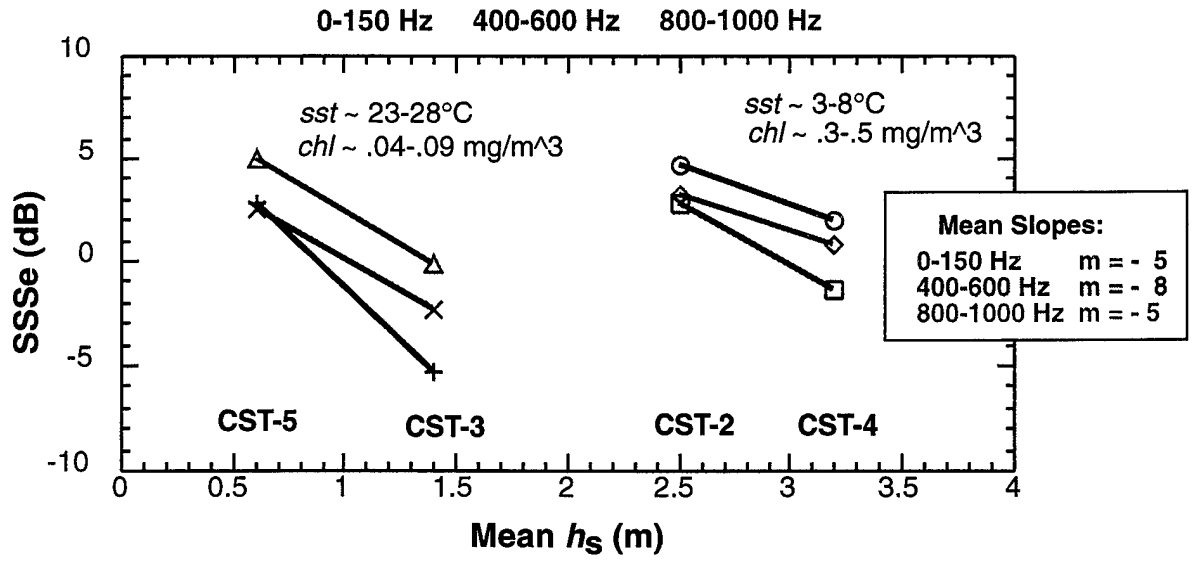

Mean regression slopes for each frequency band were used to normalize the *SSSe* averages in Table 2 for surface wave effects.

Figure 5 Influence of Background Wave Energy on Surface Scatter Strength for Sites with Similar Temperature and Chlorophyll Characteristics

where m is the average regression slope for each frequency band indicated on Figure 5 and a reference wave height of $h_{sREF} = 2.0\ m$ was chosen.

There are now two remaining variables on which *SSSn* depends: phytoplankton pigment concentration and ocean temperature. Inspection of the site environmental data in Table 2 suggests that data can be sorted into two groups: (1) a set of cold-water observations (*sst* < 11 °C) that includes CST-1, CST-2, CST-4, and CST-7; and (2) a set of low-productivity observations (*chl* < 0.3 mg/m^3) that includes CST-3, CST-5, CST-7, and Chapman-Harris. Note that only CST-7 falls into both groups.

The dependence of *SSSn* on pigment concentration for the cold-water observation set appears in Figure 6. The results imply an important role of biological activity in surface scatter. This trend is strongest at mid-frequencies (400-600 Hz). Scattering level increases (represented by decreasing *SSSn*) with biological production are probably due to higher dissolved gas levels from biological productivity and the presence of biological surfactants, both of which will extend the life of ambient bubbles.

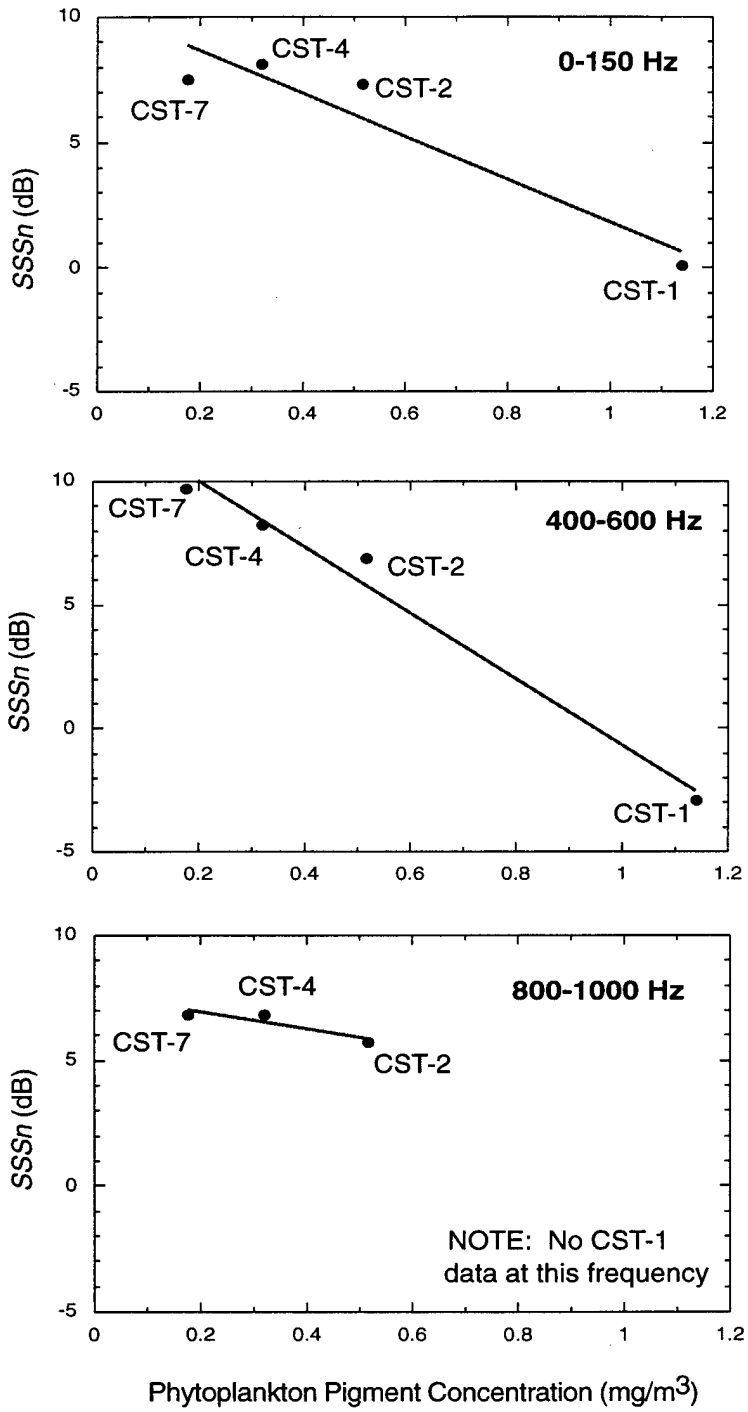

Figure 6 Influence of Biological Productivity on h_S-Normalized Surface Scatter Strength Prediction Error for the Cold Water (≤ 11°C) Observation Sites

The dependence of *SSSn* on *sst* for the low pigment observations appears in Figure 7. A definitive trend of increasing scatter (represented by decreasing *SSSn*) with increasing temperature is observed at all frequencies. These results indicate an important role of ambient ocean temperature in modulating surface scatter levels. The influence of temperature on bubble entrainment and gas dissolution results in high levels of ambient bubbles in warm water. Furthermore, near-surface stratification in warmer regions may effectively trap bubbles near the surface where the scattering effect is most important.

The results shown in Figures 5 through 7 suggest that a linear model for the dependence of *SSSe* on h_s, *sst*, and *chl* might explain a significant fraction of the site-to-site variance in SSS. The method of least-squares multiple regression was employed to test the performance of a linear model for the surface scatter prediction error

$$SSSe = \alpha h_s + \beta sst + \gamma chl + b,$$

with fit coefficients α, β, and γ for wave height, ocean temperature, and chlorophyll concentration, respectively. For the model calculations, the *SSSe* averaging was restricted to narrow wind speed, frequency, and grazing angle bands so that the results represent a specific set of environmental and acoustic conditions.

This preliminary model is quite successful in describing gross site-to-site differences in SSS. Typical results appear in Figure 8. Here the regression coefficient and the three model fit coefficients are plotted as a function of acoustic frequency at 15-25° grazing angle for the case of 8-10 m/s winds. Note that a high regression coefficient is obtained at all frequencies indicating that the model explains a large percentage of the total variance. There is a linear transition of all model parameters across frequency with the h_s and *sst* fit coefficients essentially constants.

Using α and β to normalize the data for both wave height and ocean temperature effects, as demonstrated earlier, allows a direct comparison of prediction error with phytoplankton pigment concentration. This normalization is given by

$$SSS_n = \alpha(h_{s_{REF}} - h_s) + \beta(sst_{REF} - sst) + SSSe,$$

where the reference values $h_{s_{REF}} = 2.0\ m$ and $sst_{REF} = 15°C$ were chosen. The normalized 500 Hz SSS prediction errors (*SSSn*) at each site for winds of ~10 m/s appear in Figure 9. A logarithmic fit to the data is given by

$$SSSn = -[4.8 + 3.6\log(chl)],$$

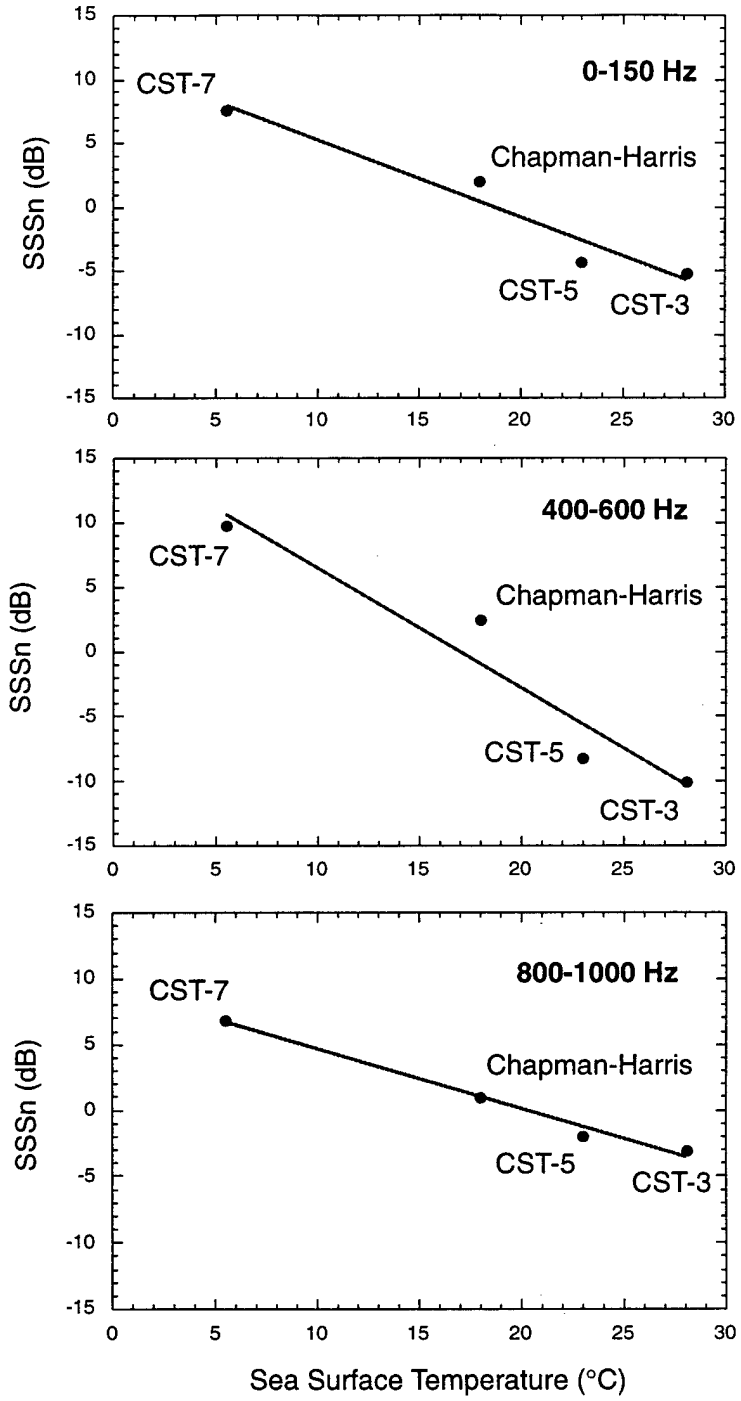

Figure 7 Influence of Ocean Temperature on h_s-Normalized Surface Scatter Strength Prediction Error for the Low Productivity ($chl \leq 0.3$ mg/m) Observation Sites

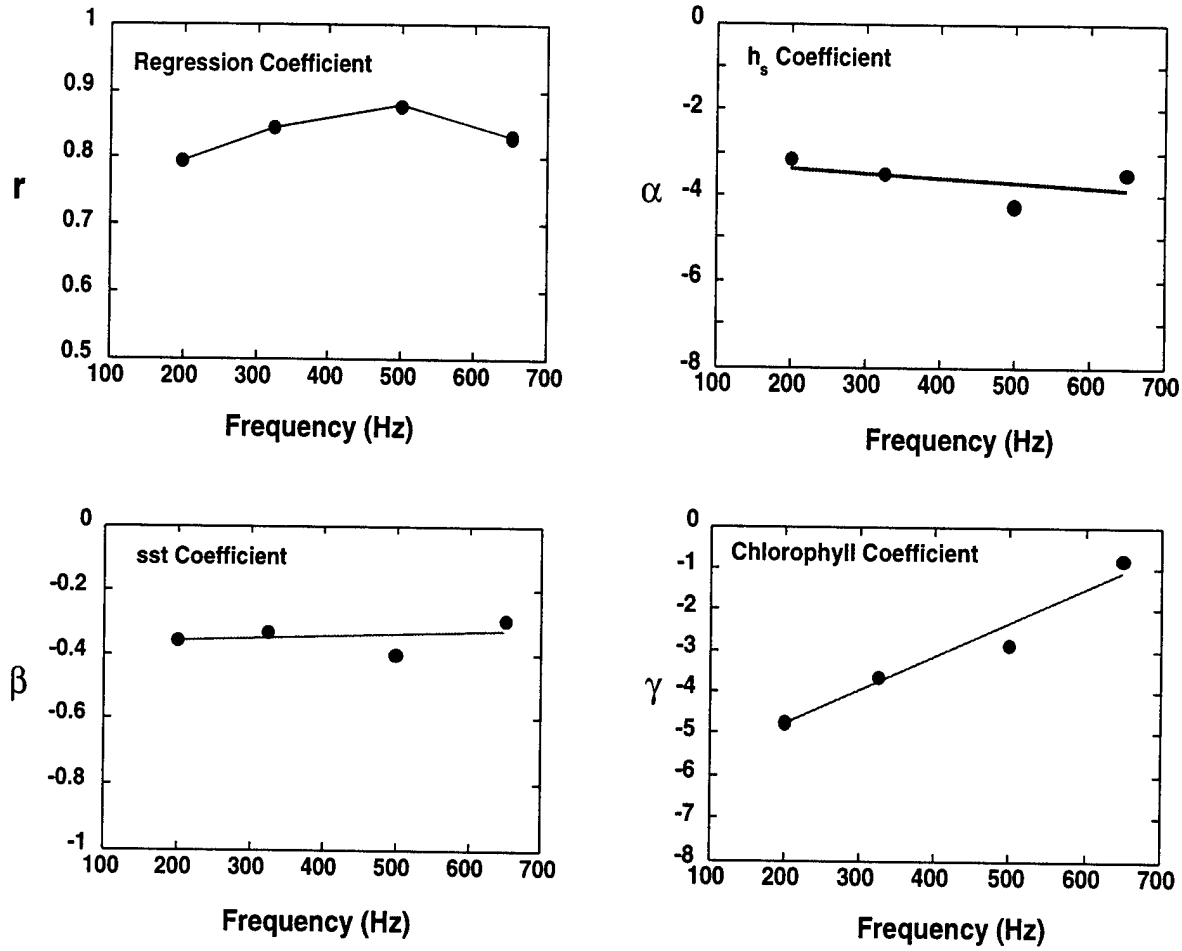

Figure 8 Multiple Linear Regression Results for the Case of U_{10} = 8-10 m/s and 15-25° Acoustic Grazing Angle

with regression coefficient $r = 0.91$. The CST-2 results are slightly farther than two standard deviations from the mean (see Figure 2) and are not included in the regression. This is perhaps due to inaccuracy of the monthly mean CZCS *chl* value in representing CST-2 conditions; inspection of the CZCS map of Figure 3 (middle panel) suggests extreme spatial variability in *chl* at that location and time. The remaining data of Figure 9 indicate that phytoplankton blooms contributed up to 5 dB in SSS site-to-site differences during CST. Extrapolating these results to nearshore phytoplankton pigment concentrations of 50 to 100 mg/m^3 indicates that SSS values can be 10 to 12 dB higher than ONE model predictions in shallow water environments.

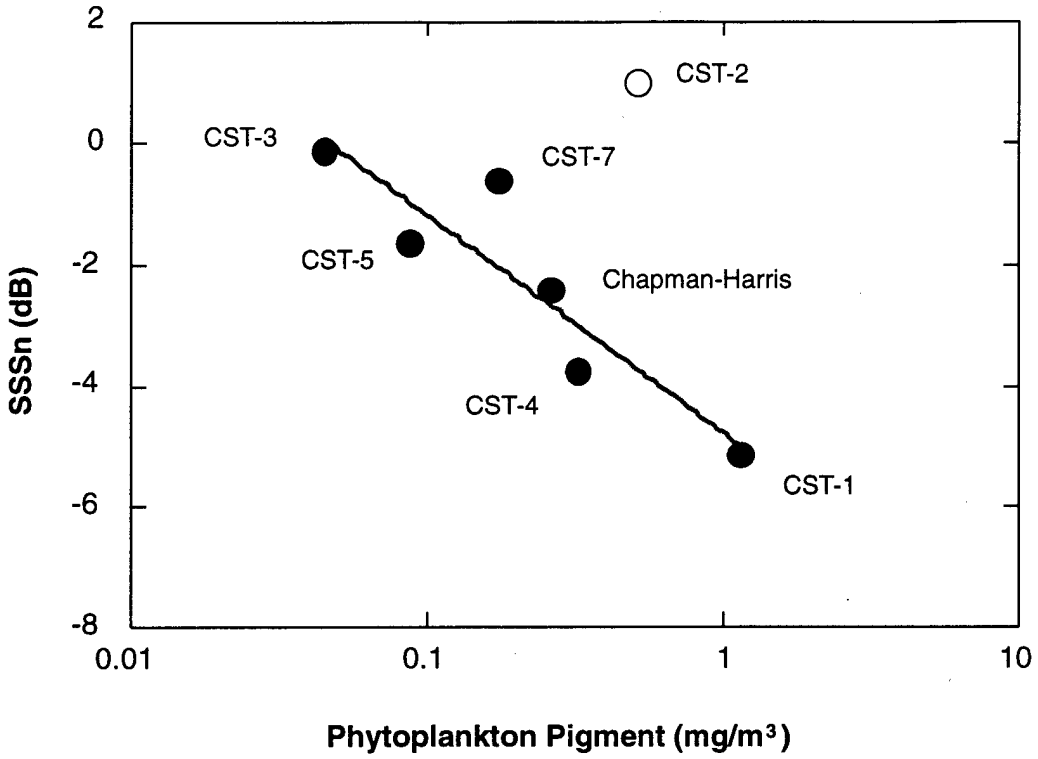

Extrapolation to nearshore conditions with *chl* ~ 50-100 mg/m^3 indicates ONE model SSS predictions can be ~ 10-12 dB too low in highly productive shallow water environments.

Figure 9 Dependence of Normalized SSS Prediction Error on Phytoplankton Pigment Concentration for an Acoustic Frequency of 500 Hz at 10 m/s winds, 20° Grazing Angle and with h_S = 2.0 m and *sst* = 15°C

5. Surface Wave Descriptors for Bubbles

The CST-7 experiment, conducted during February 1992 in the dynamic Gulf of Alaska, provided an excellent wind, wave, and whitecap observation set on which to test the hypothesis that surface wave parameters can be used to replace or augment wind speed descriptors in bubble-related air-sea process models (*Reference 3*). Wave spectral parameters were obtained from a newly developed spectral partitioning and swell tracking approach. Using these parameters, the relationships between wind forcing variability, wind sea growth, swell, and wave breaking in the open ocean were investigated.

5.1 Automated Wave Spectral Partitioning, Swell Tracking, and Storm Source Identification

To facilitate extraction of wave descriptors from directional wave spectra, we have developed a fully automated method for wave spectral partitioning, swell tracking, and storm source identification using MATLAB programming tools (*References 4 and 5*). Following an approach suggested by Susanne Hasselmann (*Reference 6*), peaks in wave buoy directional spectra are isolated based on topographic minima, with wind sea peaks identified by wave age criteria. We have added a swell tracking algorithm that provides a unique approach to storm source prediction when combined with linear wave theory. Until now, identification of swell source times and locations from wave spectra was a laborious manual procedure and limited to the dominant swell system.

Over the 6-day CST-7 wave record, 44 swell systems were identified with up to three systems coexisting at any given time (*Reference 7*). The presence of atmospheric disturbances on surface weather charts validated the storm source predictions for over 85% of these systems. A synthesis of results from the swell and wind sea separations, appearing in Figure 10, provides a distinctive representation of the surface wave history over the duration of the experiment.

The wave partitioning technique has several important applications. It would facilitate the reduction of large wave data sets such as those from satellite observations and global wave evolution models. Furthermore, the automated swell tracking and source identification procedure has a potentially important application in the forecasting of storm waves for shipping routes and populated coastal regions. In the following section, we describe how the results are used to evaluate the use of surface wave descriptors for process models related to near-surface bubble generation.

5.2 Surface Wave Dissipation and Whitecap Formation

Wave breaking is involved in many important air-sea processes, including wave energy dissipation; momentum, gas, and heat fluxes; ambient noise generation by air entrainment; radar backscatter by whitecaps; and acoustic reverberation from bubble clouds. However, the mechanisms of wave breaking in the ocean are not well understood; as a result, many of these related processes are empirically modeled using wind speed parameters (*Reference 8*). We have found that wave spectral parameters can be used in place of wind parameters in the estimation of processes related to wave breaking.

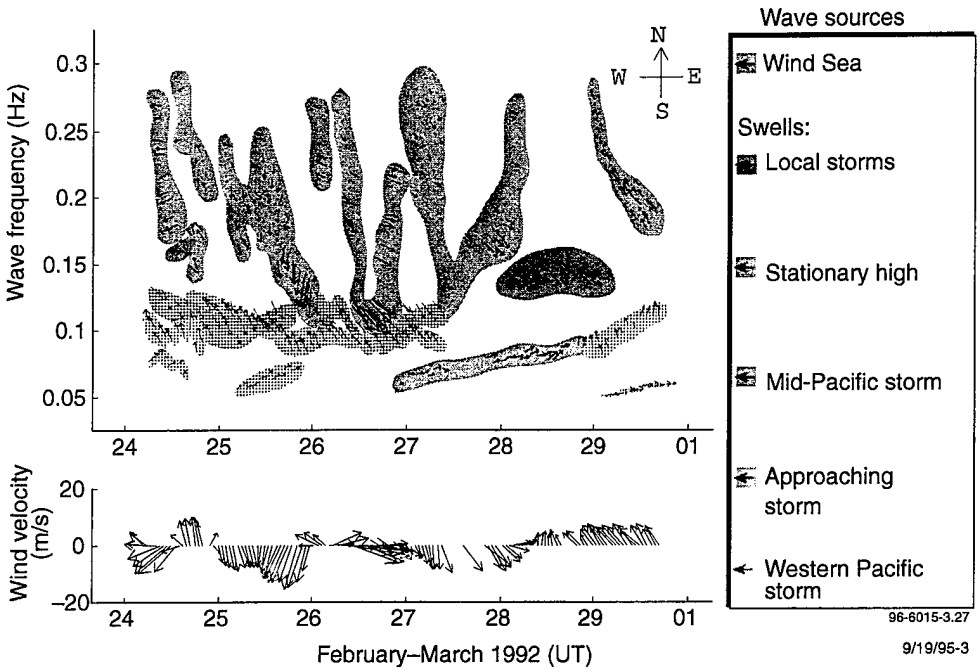

Lower panel wind vectors indicate the direction towards which the air is moving. The upper panel depicts the evolution of the principal wind sea and swell wave systems over the observation period. Wave height, direction, and frequency are represented by vector length, azimuth, and ordinate position, respectively.

Figure 10 Wind and Wave Vector History from CST-7 Gulf of Alaska Observations

The total rate of wave energy dissipation, ε_t, was estimated from the CST-7 wind sea spectral partitions using equilibrium range concepts (*Reference 9*). As demonstrated in Figure 11, replacing wind speed with dissipation rate in the standard power-law description of whitecap fraction W resulted in a new proportionality,

$$W \propto \varepsilon_t^{1.5} \ ,$$

which reduces the scatter of W about the independent variable by 2 to 3 orders of magnitude. These improvements result primarily from the removal of wind trend effects that add uncertainty to wind speed relationships. The successful description of whitecaps by our dissipation rate estimates lends credibility to the equilibrium range theory as a viable approach to modeling bubble generation by wave breaking.

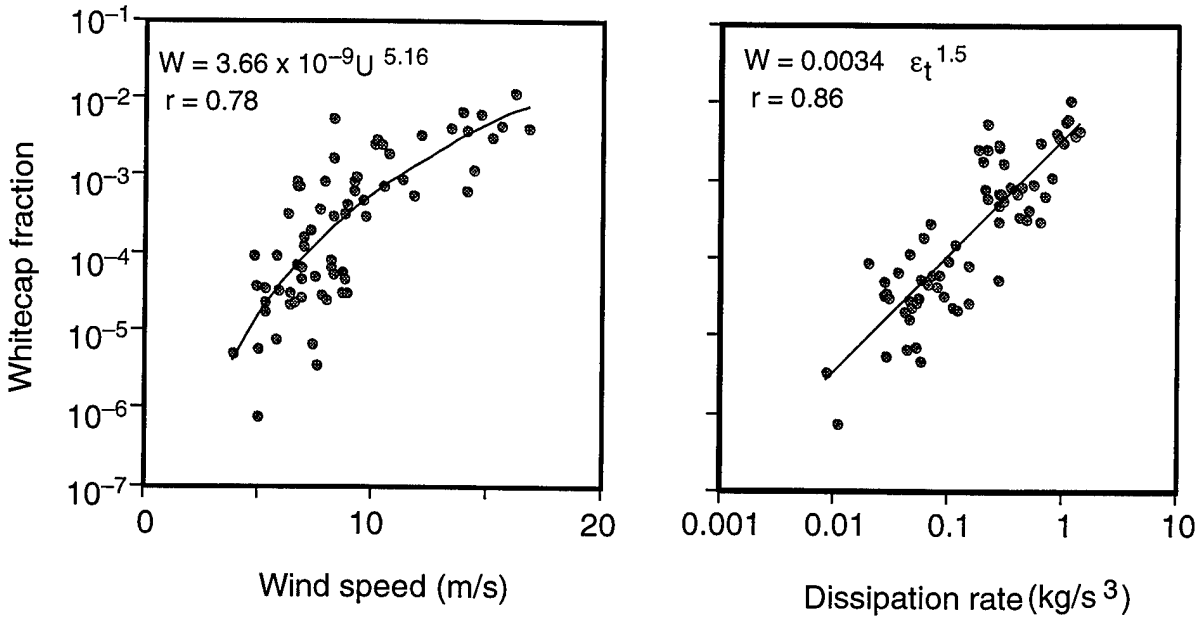

Wave dissipation rate reduces the scatter about a power-law model.

Figure 11 Dependence of Whitecap Fraction on Wind Speed and Wave Dissipation Rate

Remote sensing techniques, wave buoy arrays, and regional wave modeling efforts are continually being refined so that soon high-quality directional wave spectra will be routinely available on a global scale. It is conceivable that air-sea process models for such mechanisms as gas flux, radar backscatter, underwater ambient noise, and near-surface acoustic reverberation will soon improve significantly due to the use of surface wave spectral parameters in place of external forcing parameters. Since wave-related processes are dynamically linked to intrinsic properties of the wave field, the use of wave parameters should improve model performance.

6. Conclusions and Recommendations

6.1 Conclusions

- Gross site-to-site differences in SSS are explained by seasonal and geographic environmental factors.
- Biological productivity significantly increases SSS in the open ocean. This is likely due to increased dissolved gas levels and the presence of biochemical surfactants, both of which will extend bubble lifetimes. This effect will be amplified in shallow water environments.

- SSS is higher in warm water. This is likely a result of greater bubble supply due to viscosity and surface tension effects and decreased gas solubility which acts to extend bubble lifetimes. Increased temperature variability will greatly influence scattering strength statistics in shallow water environments.
- SSS increases in higher-energy environments. Here the background ocean energy level was characterized by significant wave height averaged over several days.
- Wave spectral partitioning can be employed to extract wave descriptors for bubble-related processes in the ocean.
- Wave dissipation rate improves the standard power-law model for the prediction of ocean whitecaps.

6.2 Recommendations for Continued Research

- Prepare a robust SSS model with physical and biological parameters for site-to-site variability
- Determine the relevance to other SSS observation sets including ASREX
- Estimate SSS statistics for various shallow water strategic areas of interest

7. Acknowledgments

Valuable discussions with Alan Brandt, Fred Erskine, David Farmer, Scott Hayek, Frank Henyey, Ken Melville, Owen Phillips, John Sweeney, Eric Thorsos, and Svein Vagle helped shape the hypotheses leading to these results. Environmental and acoustic data were provided by Rick Marsden, Ed Monahan, Mike Nicholas, Pete Ogden, and Larry White. An early version of the wave partitioning code was supplied by Susanne Hasselmann. Mike Mandelberg contributed to the data assimilation, organization, and preliminary analyses.

8. Reports and Publications Resulting from this Grant

Hanson, J. L., 1996. "Wind Sea Growth and Swell Evolution in the Gulf of Alaska," Ph.D. Dissertation, The Johns Hopkins University.

Hanson, J. L., 1996. "Wave Spectral Partitioning Applied to the Analysis of Complex Wave Conditions in the North Pacific Ocean," *Eighth Conference on Air-Sea Interaction*, The American Meteorological Society, pp. 61-65.

Hanson, J. L., 1997. "Assimilation of Surface Wave Spectral Parameters for Air-Sea Flux Modeling," *Annales Geophysicae*, **15**(Supple. II), European Geophysical Society, pp. C406.

Hanson, J. L. and M. D. Mandelberg, 1996. "Surface Wave Parameters for the Prediction of Breaking Waves and Acoustic Backscatter," *J. Acoust Soc Am*, **100**(4) part 2, pp. 2806.

Hanson, J. L. and O. M. Phillips, "Measurements of the Spectral Evolution of Surface Wave Fields in the Gulf of Alaska Using Wave Spectral Partitioning," subm. *J. Geophys. Res.*

Hanson, J. L and O. M. Phillips, "Wind Sea Growth and Dissipation in the Open Ocean," subm. to, *J. Phys. Ocean.*

Kline, S. A. and J. L. Hanson, 1995. "Wave Identification and Tracking System," Johns Hopkins University Applied Physics Laboratory Technical Report STD-R-2436.

Liu, E., 1997. "Linear Multivariate Analysis of CST and ASREX Observations," Johns Hopkins University Applied Physics Laboratory Technical Memorandum STF-97-013 (Summary of Work Performed at JHU/APL, January 6 through January 24).

Mandelberg, M. D. and A. R. Schneck, 1996. "ASREX and Historical Oxygen Saturation," Johns Hopkins University Applied Physics Laboratory Technical Memorandum STF-048-96.

REFERENCES

1. Chapman, R. P., and Harris, J. H., *J. Acous. Soc. Am.*, **34**(10), pp. 1592-1597, (1962).

2. Wu, J., "Individual Characteristics of Whitecaps and Volumetric Description of Bubbles," *IEEE J. Oce. Engineering*, **17**(1), pp. 150-158, (1992).

3. Hanson, J. L., "Wind Sea Growth and Swell Evolution in the Gulf of Alaska," Ph.D. Dissertation, The Johns Hopkins University, 1996.

4. Hanson, J. L., "Wave Spectral Partitioning Applied to the Analysis of Complex Wave Conditions in the North Pacific Ocean," Eighth Conference on Air-Sea Interaction, The American Meteorological Society, pp. 61-65, 1996.

5. Kline, S. A. and Hanson, J. L., "Wave Identification and Tracking System, The Johns Hopkins University Applied Physics Laboratory Technical Memorandum STF-97-013, 1995.

6. Hasselmann, S., in Komen et al., *Dynamics and Modeling of Ocean Waves*, Cambridge University Press, 1994.

7. Hanson, J. L. and Phillips, O. M., "Measurements of the Spectral Evolution of Surface Wave Fields in the Gulf of Alaska Using Wave Spectral Partitioning," subm. to *J. Geophys. Res.*, September 1997.

8. Hanson, J. L., "Assimilation of Surface Wave Spectral Parameters for Air-Sea Flux Modeling," *Annales Geophysicae*, **15** (Suppl. II), European Geophysical Society, pp. 6406, 1997.

9. Hanson, J. L. and Phillips, O. M., "Wind Sea Growth and Dissipation in the Open Ocean," subm. to, *J. Phys. Ocean*, October 1997.

This page intentionally left blank.

THE JOHNS HOPKINS UNIVERSITY
APPLIED PHYSICS LABORATORY
LAUREL, MARYLAND

EXTERNAL DISTRIBUTION FOR STD-R-2694

Office of Naval Research
800 North Quincy Street
Arlington, VA 22217-5660
ATTN: Jeff Simmen (Code 321OA)
Eddie Estalote (Code 3210A)
Note: (3 copies)

Director, Naval Research Laboratory
ATTN: Code 2627
4555 Overlook Drive
Washington, DC 20375-5326

Charles Bohman
Program Executive Officer
Air ASW Assault and Special Mission Program
PMA 2992B
47123 Buse Road, Unit # IPT
Patuxent River, MD 20670-1547

Defense Technical Information Center
8725 John J. Kingman Road
STE 0944
Ft. Belvoir, VA 22060-6218
Note: (2 copies)

Naval Research Laboratory
Washington, DC
20375-5350
ATTN: Roger Gauss (Code 7144)
Fred Erskine (Code 7142)
Mike Nicholas (Code 7145)
Daniel Wurmser (Code 7144)

The Johns Hopkins University
34th and Charles Street
Baltimore, MD 21218
ATTN: Owen Phillips
Andrea Prosperetti

Jennifer Barron
105 Ames Hall
The Johns Hopkins University
Baltimore, MD 21218

Applied Physics Laboratory
University of Washington
1013 NE 40th Street
Seattle, WA 98105
ATTN: Frank Henyey
Eric Thorsos
Jeff Nystuen
Peter Dahl

Institute of Ocean Sciences
P.O. Box 6000
9860 West Saanich Road
Sidney, British Columbia
CANADA V8L 4B2
ATTN: David Farmer
Svein Vagle

Rosentiel School of Marine and
Atmospheric Science
University of Miami
4600 Rickenbacker Causeway
Miami, FL 33149-1098
ATTN: Harry DeFerrari
Neil Williams

Applied Research Laboratory
Pennsylvania State University
State College, Pennsylvania 16804
ATTN: Ken Gilbert

Scripps Institution of Oceanography
University of California, San Diego
La Jolla, CA 92093-0213
ATTN: W. Ken Melville

Woods Hole Oceanographic Inst.
Woods Hole, MA 02543
ATTN: Eugene Terray

This page intentionally left blank.